Pole shape influence of an automotive alternator: Magnetic noise minimization.

HECQUET Michel, GOUEYGOU Marc, AIT-HAMMOUDA Amine, BROCHET Pascal.

L2EP - Ecole Centrale de Lille, BP 48, 59651 Villeneuve D'Ascq, FRANCE
Michel.hecquet@ec-lille.fr, Marc.goueygou@ec-lille.fr, Pascal.brochet@ec-lille.fr

Abstract **-- A numerical procedure to optimize the pole shape of an automotive alternator is presented. This alternator is a claw-pole machine, that is modelled by an electrically coupled permeance network. Saturation, electronic commutations and rotor movement are take into account. Noise and vibration are important quality factors of the alternator and are mostly due to electromagnetic phenomena. Some geometric parameters of the claw are investigated and the Experimental Design Method is used to find a global optimum that would minimize vibration and noise levels. Consequently, numerical simulations and measurements are carefully compared, so as to validate the numerical procedure. A correlation between radial force, torque and vibration harmonics is also established.**

1. Introduction

Nowadays, the three dimensional (3D) finite element method (F.E.M.) is used to study typical machines, for example, an automotive alternator [1], [2]. However, a complete study requires a coupling with electrical circuits (rectifier and battery). Moreover, if the movement is taken into account, a prohibitive computation time is necessary [1], [3]. Hence, the optimization of this alternator shape is very difficult.

In order to address this problem, a modeling approach based on a magnetic and electric coupled network is proposed. The magnetic circuit of the machine is modelled by a permeance network, where permeances are identified by 3D magnetostatic finite element calculations. Then, the coupling of this network to electrical circuits and powers electronics is performed [4].

This approach has already been tested and validated on two different alternators. Different results (flux, electromotive forces, currents) were compared with experimental measurement [5], [6].

The computing magnetic forces for several speeds and different currents have been determined. These results are compared with those obtained by 3D magnetostatic finite element calculations [6], [7]. They have shown that the 3D permeance network model provides quickly the temporal variation of forces with a good accuracy.

After a presentation of the pole shape study, the approach to minimize the harmonic of radial forces is described. The Experimental Design method is used jointly with numerical simulations in order to identify the optimal claw-pole parameters.

Secondly, in order to validate the procedure, particularly its capability to give the correct variation of the studied responses when varying the pole shape, tests and measurements are made on specifically re-carved.

2. Claw-Pole Alternator

The distinctive feature of this machine is that the field winding is composed of only one excitation coil enclosed by two pole wheels, or claw-pole. The flux concentration is greater in the claw-pole base, resulting in an axial flux machine called 'Modified Lundell Alternator'(fig.1 a).

3. 3D Permeance Network

A bounded permeance network taking into account geometric and electric periodicity is used to model the magnetic circuit of the machine. Each part of the magnetic circuit is represented by its permeance [8]. The network topology is chosen according to geometric considerations based on a knowledge of the general direction of the flux tubes. In order to determine the main and leakage permeances, a 3D magnetostatic finite element analysis is used [9]. The effect of saturation is taken into account by introducing flux-dependent permeances, using the standard B(H) curve of the material.

In order to take into account the rotor movement, the air-gap permeances (Pe) located between each stator tooth and claw-pole nodes are defined. The evolution of air-gap permeances with mechanical angle θ is established using 3D magnetostatic finite elements for several positions of the stator and the rotor. Then, a trigonometric interpolation is used to obtain a continuous law with continuous first derivative. In this way, the permeance network is determined for any rotor position, as shown in figure 1.

Next, this network is coupled with internal and external electric circuits. The three output phases are connected to a six-diode rectifier and a resistive load. The alternator produces three alternating currents, which are the origin of the magnetomotive forces in the magnetic circuit of the stator. To establish the relationship between the electric current and the magnetomotive forces in the stator, a closed loop around each slot is considered, with a magnetomotive force (F_i) associated to each tooth (i), as shown in figure 1.

Finally, applying Ampere's law to this loop, a system of equations, as in 1, for calculating the magnetomotive forces is derived.

$$F_{(i+1)} - F_{(i)} = -N_s I_i \qquad i = 1, n_e \qquad (n_e\text{:tooth number}) \qquad (1)$$

Hence, a complete model is obtained. It includes the supply, the magnetic circuit with the air-gap permeances and the load [4] (fig.1).

Fig. 1 a : Claw-pole alternator

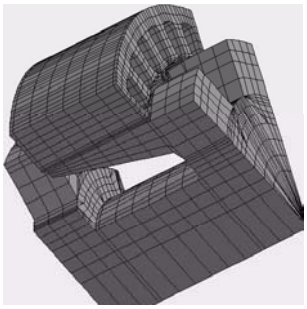

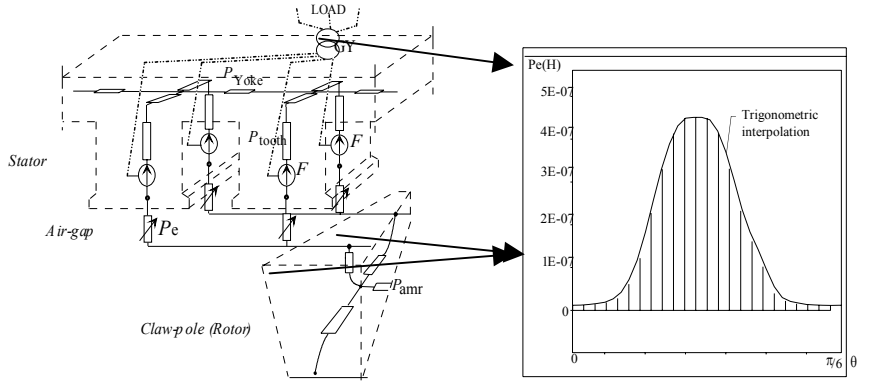

Fig.1 : A part of 3D-permeance network.
*P*e, the air-gap permeances, *F,* the magnetomotive force source, *P*amr, the armature magnetic reaction and GY, the element for coupling the stator and the electrical load.

4. Simulation Results

The resulting model has been validated on several experiments [4], [5], [6]. It provides the time-dependent variation of the stator tooth flux, of electromotive forces (EMF), current, electromagnetic torque and magnetic forces applied to a stator tooth. For example, the radial force variation for different speeds is presented in [6].

The influence of the armature magnetic reaction can be seen on these figures. The same results can also be obtained using a finite element method [1], [2], but the main advantage of the permeance model is the very small computation time, two minutes per period, thus allowing the geometry of this complex machine to be otimized.

In the following section, the optimization process of the claw-pole shape is presented.

5. Numerical and Experimental Study of the Pole Shape

In this section, some geometric parameters of the claw-poles only are investigated because the pole shape is easily modified. In particular, their influence on the alternator's response in terms of stator electromotive forces (emf), radial forces, torque and vibrations is presented.

The Experimental Design Method can be used in two ways [10], [11]: Screening to determine what are the significant parameters and Response Surface Methodology to build an accurate analytical model.

In our case, three parameters, as shown in figure 2, are known to be significant: 'L' width of claw base, 'l' width of claw tip and 'lg' claw length and certainly with non-linear effects.

In this paper, this three parameters are named 'para1', 'para2' and 'para3'.

As a first step, different parameters of the claw were investigated and the Screening approach has been applied on experimental measurements.

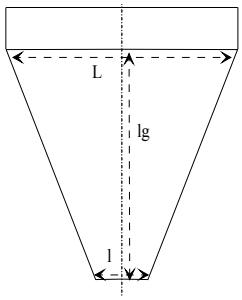

Fig.2: parameters of the claw-pole.
L : width of claw base, l : width of claw tip, lg: length

5.1. Parameter variations with the permeance network approach:

In order to take into account the variation of claw pole geometry, a parameterised model is developed [7]. The overall procedure is automated by a supervisor, presented in figure 3. Using script files [9], a parameterized finite element model is defined in the pre-processor and the post-processor is customized to give new values of air-gap permeance and circuit permeances. These are then introduced in the permeance network simulator to obtain different results (emf., current, flux...) and its spectrum. With this structure miscellaneous mistakes are avoided and evaluation of each test is very quick, twenty minutes to execute all the steps.

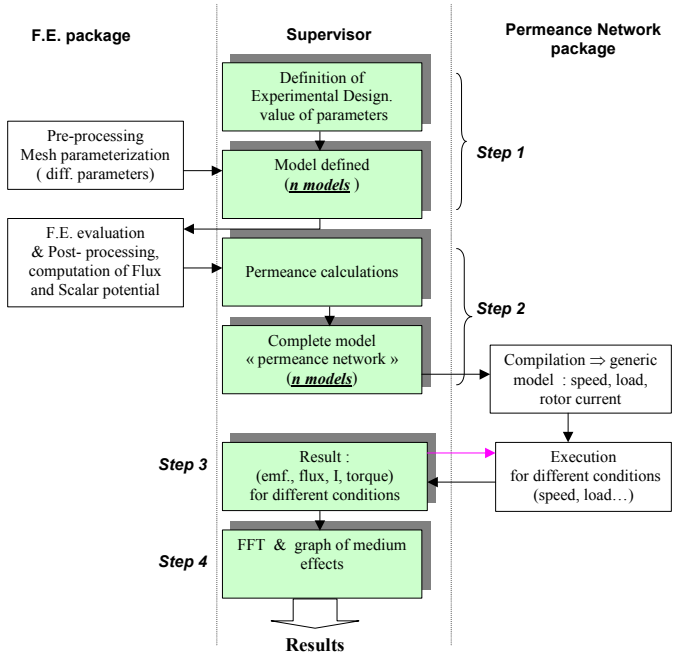

Fig.3: Different steps of the permeance network design and simulation

Hence, many simulations can be done with parameter variations of the claw-pole that are equal to a few millimeters.

In addition, rotors have been specifically built to validate experimentally the simulation results, but only the min and max values of parameters were used, as shown in figure 4.b.

In order to minimize the influence of assembling and eccentricity, a particular test bench has been designed. As a matter of fact, assembling of the rotor, even for identical rotors, can have an major influence on vibration measurements.

5.2 Electrical measurements and simulations:

The first response to be studied is the stator electromotive force for a rotation speed of 3000 rpm, a maximum field current and no load (figure 4). The bar graphs of figures 4 and 5 show the effects of each of the three possible values of the geometric parameters on the ratio between the amplitude of third harmonic of emf and the amplitude of the first one.

The main effects, for example for the parameter $para3_{max}$, is determined by this relation [10]: Y = I+ Y1+Y2+Y3+Y4.....

- I : the mean value of all experiments
- Yi : the response only for para3 is maximum.

In order to verify our representation fig.4a and 5a, the addition of different main effects is equal zero. This verification is possible in simulations only because a some rotors built for experimental measurements were missing and orthogonality property is not respected.

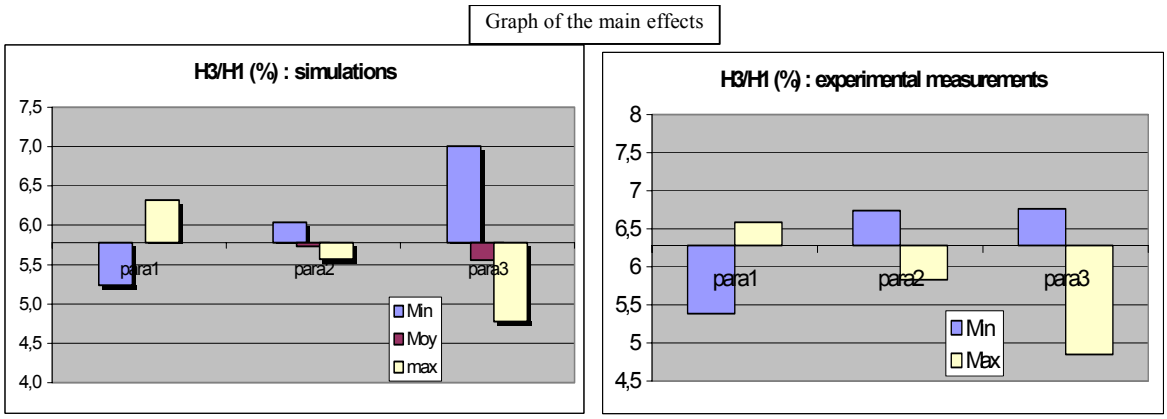

(a) Simulations (b) Measurements

Fig. 4 : stator electromotive forces **on no-load**.
Min., Moy. And max. : different values of parameters

Experimental results well agree with numerical simulations.

With these graphs the best choice is obvious : on no-load, the third parameter is the most significant to minimize the third harmonic. In addition, in order to reduce this harmonic, para3 must be maximum, para1 minimum, and para2 maximum.

Simulations and measurements are also compared on load, including a rectifier and a resistor with an output current of 75A, fig.5. They display the same trends but surprisingly the second parameter becomes the most influential. This may be explained by the armature magnetic reaction, which may change the effect of each parameters.

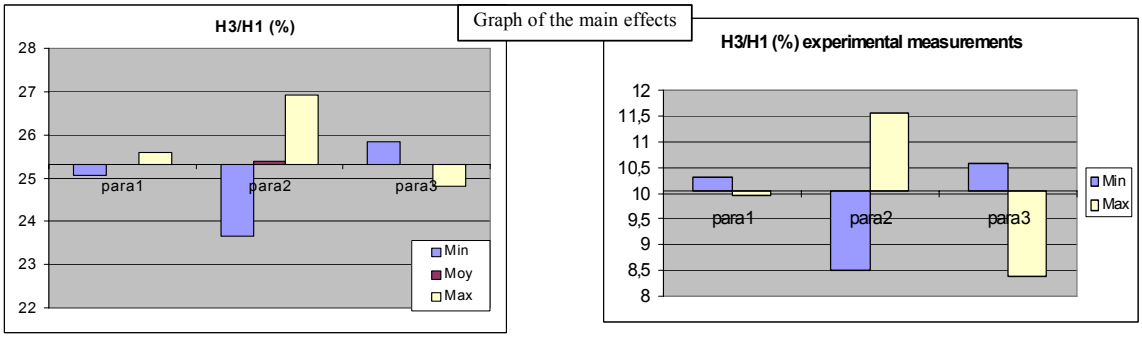

(a) Simulations (b) Measurements

Fig. 5 : stator electromotive forces **on load (rectifier and resistor)**

The same trends are observed on the 6th harmonic (H6) of the electromagnetic torque, as shown in figure 6. This harmonic corresponds to the slot effect and its detailed in the part C.

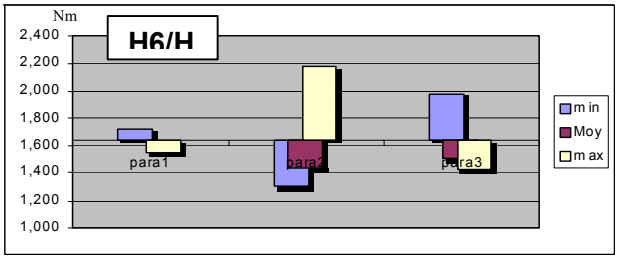

Fig. 6 : electromagnetic torque (H6/H1) on load
Rem. : H6 varies between 5 to 12% of H1.

As a conclusion for this section, similar trends were obtained for simulations by the permeance network approach and for experimental measurements, validating this approach.

For example, in the "on-load" case, factor 1 is negligible and factor 2 (para2) is predominant :

- *para2 must be minimum,*
- *para3 must be maximum.*

} "on-load" case

Hence, in order to verify this trend, a comparison was made with vibration and acoustic measurements.

5.3. Acoustic and vibration measurements :

Several measurements were made for each rotor. We only present vibration and acoustic measurements for three rotors with the extreme values of the geometric parameters :

- rotor (a): para2 is minimum and para3 maximum,
- rotor (b): para2 is moy. and para3 minimum,
- rotor (c): para2 is maximum and para3 minimum.

The rotor (a) and (c) are expected to display opposite trends.

An accelerometer is placed directly on the stator to record its vibrations. A microphone is connected to a spectrum analyzer to record the acoustic noise. Different locations for these sensors were tested. The measurement conditions are : maximum field current i_{ex}, six-diode rectifier and resistor connected, 75A stator phase current, and N =3000rpm.

In addition, one rotor was taken out and re-assembled several times, and vibration measurements were made to check the effect of assembling.

In figure 7, a vibration spectrum is presented for one rotor and in tab.1, the level of vibration harmonics for different rotors : a, b and c.

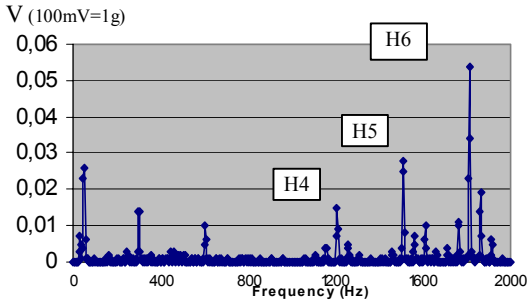

Fig. 7 : Vibrations harmonics measurements.

Table 1 : Vibration harmonics measurements for three rotors

Rotor type / harmonic number	H1	H4	H5	H6
Rotor (a) (V)	0.021	0.003	0.011	0.025
Rotor (b) (V)	0.028	0.005	0.07	0.030
Rotor (c) (V)	0.026	0.015	0.028	0.058

The 6th harmonic (H6) is the most important for this measurement setup. Its frequency is 1800Hz for N=3000rpm, thus corresponding to the slot frequency :

$$Fs = 6\ m\ f\ = 1800Hz$$

with m = 1 : number of slot/pole/phase and f = fundamental frequency = 300Hz .

In the tab.2 and figure 8, levels of acoustic noise harmonics are presented:

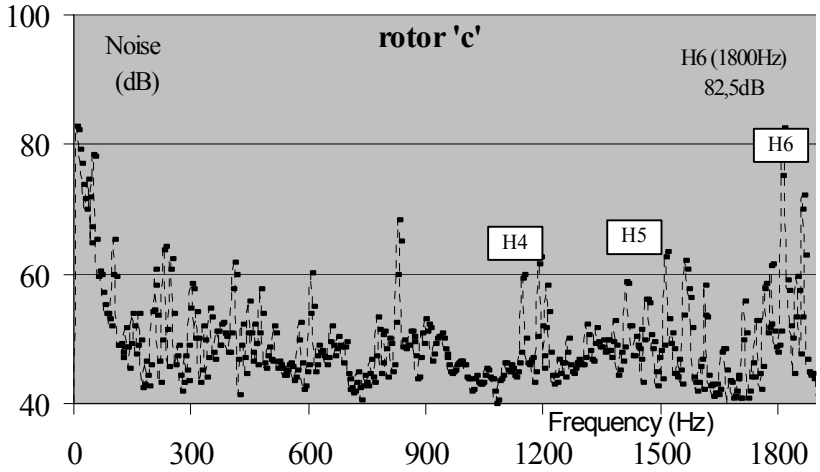

Fig. 8 : levels of acoustic noise harmonics only for ROTOR 'c'

Table 2 : Acoustic noise measurements for three rotors

Rotor type / harmonic number	H1	H4	H5	H6
Rot. (a) (dB)	52	62	65.5	70.2
Rot. (b) (dB)	53	63.5	60.8	75.8
Rot. (c) (dB)	57	60	62.1	82.5

The maximum acoustic noise level is obtained for 6^{th} harmonic H6 (1800Hz) and for the rotor (c). In comparison with the simulation part, the same trends are obtained and the rotor (a) gives better results.

6. Conclusion

The proposed approach that is the application of the Experimental Design Method to numerical model obtained by connecting a permeance network with an electric network, has been successfully tested. This approach has been also confirmed by measurements on a test bench.

A numerical procedure to optimize the pole shape of on automotive alternator is presented. In order to minimize vibrations and noise level, a tendency of the claw-pole shape is given. This efficiency of this design has been confirmed by numerical results and experiments.

In addition, the structure of the test bench warrants the reproducibility of measurements when mounting and dismounting the rotors. Future investigations are necessary to test all rotors and to increase the optimization of the complete model.

7. References

[1] I. Ramesohl, G.Henneberger, S. küppers and W. Hadrye, "Three dimensional calculation of magnetic forces and displacements of a claw-pole generator ", IEEE Trans. on Magnetics, May 1996, Vol. 32, N°3, pp1685-1688.

[2] Ramesohl I, T.Bauer and G.Henneberger, 'Calculation procedure of the sound field caused by magnetic excitations of the claw-pole alternator' ,Vibrations and Noise of Electric Machinery, Béthune , May 98, France, pp102-108.

[3] T. Dreher, "Couplage de la méthode des éléments finis tridimensionnels avec une méthode d'analyse du circuit électrique : application à la modélisation des machines électriques tournantes", Thesis, Institut National Polytechnique de Grenoble, Oct 1994.

[4] M. Hecquet , " Contribution à la modélisation des systèmes électrotechniques par la méthode des schémas équivalents magnétiques. Application à l'alternateur automobile", Thesis, Sciences and Technology University of Lille, January 1995.

[5] M. Hecquet, P. Brochet, "Modélisation d'un alternateur automobile par un réseau de perméances couplé à des circuits électriques ", Journal of applied Physics. III, August 96, pp 1099-1116.

[6] M. Hecquet, P. Brochet, "Time variation of forces in a synchronous machine using electric coupled network model", IEEE Trans. on Magnetics, Vol.34, N°5, pp 3214-3217, Sept. 98.

[7] M. Hecquet, S. Dahel, M. Goueygou, P. Brochet, 'Numerical computation of pole shape influence on radial forces in an automotive alternator', Vibrations and Acoustic Noise of electric Machinery Lodz, Pologne, June 2000, pp108-113.

[8] Ostovic V., "Dynamics of saturated machines", Springer-Verlag, 1989.

[9] Opera-3D, Vector Fields software, reference manual.

[10] J. Goupy, ' La Méthode des plans d'Expériences', Dunod, Paris, 1988

[11] F. Gillon, P.Brochet, 'Optimisation of a Brushless Permanent-Magnet Motor with the Experimental Design Method', IEEE Trans. on Magnetics, Sept. 1998, Vol. 34, N°5, pp 3648-3651